Proceedings of 6th Thin Film Materials & Devices Meeting
November 2-3, 2009, Kyoto, Japan
http://www.tfmd.jp/

Transistor Characteristics and Thermopower Modulation of $KTaO_3$ Single Crystal Based Field-Effect Transistors with *a*-C12A7 Gate Dielectric

Akira Yoshikawa[1], Kosuke Uchida[1], Kunihito Koumoto[1], Takeharu Kato[2], Yuichi Ikuhara[2,3], Hiromichi Ohta[1,4]

[1] Graduate School of Engineering, Nagoya University, Chikusa, Nagoya 464-8603
[2] Japan Fine Ceramics Center, Atsuta, Nagoya 456-8587
[3] Institute of Engineering Innovation, The University of Tokyo, Yayoi, Bunkyo113-8656
[4] PRESTO, Japan Science and Technology Agency, Honcho, Kawaguchi 332-0012

Keywords: $KTaO_3$, amorphous C12A7, field modulation, thermopower

Abstract. We show herein fabrication and field-modulated thermopower for $KTaO_3$ single-crystal based field-effect transistors (FETs). The $KTaO_3$ FET exhibits field effect mobility of ~8 $cm^2V^{-1}s^{-1}$, which is ~4 times larger than that of $SrTiO_3$ FETs. The thermopower of the $KTaO_3$ FET decreased from 600 to 220 μVK^{-1} by the application of gate electric field up to 1.5 $MVcm^{-1}$, ~400 μVK^{-1} below that of an $SrTiO_3$ FET, clearly reflecting the smaller carrier effective mass of $KTaO_3$. The thermoelectric power factor of $KTaO_3$ was estimated to be ~1.5 $mWm^{-1}K^{-2}$ at room temperature, which is approximately 50 % for that of $SrTiO_3$.

Introduction

Thermoelectric energy conversion technology attracts attention to convert the waste heat into electricity.[1] Generally, the performance of thermoelectric materials is evaluated in terms of a dimensionless figure of merit, $ZT = S^2 \cdot \sigma \cdot T \cdot \kappa^{-1}$, where Z, T, S, σ and κ are a figure of merit, the absolute temperature, the thermopower, the electrical conductivity, and the thermal conductivity, respectively. Today, thermoelectric materials with $ZT > 1$, which is necessary for practical applications, are being rigorously explored though the ZT values of several materials such as Bi_2Te_3 and PbTe exceed 1 because these materials are not attractive, particularly operating at high temperatures (T~1,000K). Further, the use of these heavy metals should be limited to specific environments such as space because they are mostly toxic, low in abundance as natural resources, and thus not environmentally benign. Based on this background, recently, metal oxides such as layered cobaltates [2] and electron doped $SrTiO_3$ [3] attract much attention for thermoelectric power generation material at high temperatures on the basis of their potential advantages over heavy metallic alloys in chemical and thermal robustness.

Thermoelectric materials are explored mostly using charge carrier-doped semiconductors with various doping levels because the $S^2 \cdot \sigma$ value must be enhanced according to the commonly observed trade-off relationship between two material parameters in terms of charge carrier concentration (n): σ increases almost linearly with increasing n until ionized impurity scattering or electron-electron scattering becomes dominant, while $|S|$ decreases with n. Therefore, a great deal of material is needed to optimize thermoelectric properties.

Very recently, Sakai *et al.*[4] reported thermoelectric properties of several Ba-doped $KTaO_3$ single crystals ($n = 5.4 \times 10^{18} - 1.4 \times 10^{20}$ cm^{-3}). They found that heavy (>10^{20} cm^{-3}) electron doping in $KTaO_3$ would provide large thermoelectric properties. $KTaO_3$ (S.G.: *Pm3m*, lattice parameter a = 3.989 Å) is a typical band insulator with a large band gap of ~3.8 eV.[5] Metallic

conductivity in $KTaO_3$ can be obtained by the appropriate impurity doping [6] and/or the introduction of oxygen vacancies.[7-9] $KTaO_3$ exhibits very high Hall mobility of $>10^4$ $cm^2V^{-1}s^{-1}$ at 2 K.[10] Since these physical properties of $KTaO_3$ are similar to those of $SrTiO_3$,[11,12] which exhibits largest *ZT* among transition metal oxides (*n*-type), $KTaO_3$ would be promising candidate for thermoelectric application.

In order to examine the thermoelectric properties of *S* and σ for $KTaO_3$, we fabricated a field effect transistor (FET) structure on a single crystal $KTaO_3$ because a FET structure on single-crystalline material would be a powerful tool in optimizing thermoelectric properties because it provides the charge carrier dependence of both *S*- and σ-values simultaneously.[13] Here we report the fabrication and thermopower modulation of the $KTaO_3$ FET. The resultant $KTaO_3$ FET exhibits excellent transistor characteristics: on-off current ratio of ~10^5, sub-threshold swing S-factor of 1.2 $Vdecade^{-1}$, threshold gate voltage V_{th} of +5.2 V, and field effect mobility μ_{FE} of ~8 $cm^2V^{-1}s^{-1}$. The thermopower $|S|$ of this $KTaO_3$ FET can be modulated from 600 to 220 μVK^{-1} by the application of gate electric field up to 1.5 $MVcm^{-1}$. The thermoelectric power factor $S^2 \cdot \sigma$ of $KTaO_3$ was estimated to be ~1.5 $mWm^{-1}K^{-2}$ at room temperature, which is approximately 50 % for that of $SrTiO_3$.

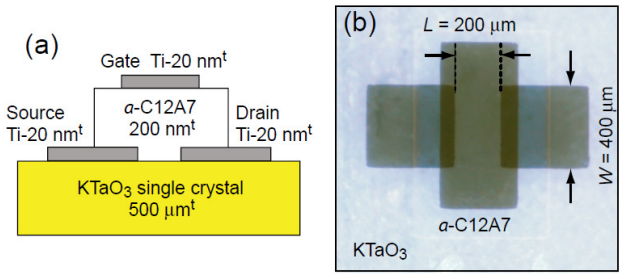

Fig. 1: (a) The schematic device structure and (b) a photograph of the $KTaO_3$ FET. Ti films (20-nm thick) are used as the source, drain and gate electrodes. A 200-nm thick *a*-C12A7 film is used as the gate insulator. Channel length (*L*) and channel width (*W*) are 200 and 400 μm, respectively.

Experimental

The schematic structure and photograph of the $KTaO_3$ FET are shown in Figs. 1(a) and 1(b), respectively. First, we treated (001) $KTaO_3$ single crystal plates (10 × 10 × 0.5 mm, SHINKOSHA Co.) with buffered NH_4F-HF solution (BHF, pH = 4.5) to obtain an atomically smooth surface [14] because atomically smooth heterointerface of the gate insulator/oxide may be necessary for FET fabrication.[15] The NH_4F concentration was kept at 10 mol/*l*. After the BHF treatment, we obtained a relatively smooth surface with steps (~0.4 nm) and terraces [Fig. 2(b)] as compared to an untreated surface [Fig. 2(a)]. Second, 20-nm-thick metallic Ti films, which would serve as source and drain electrodes, were

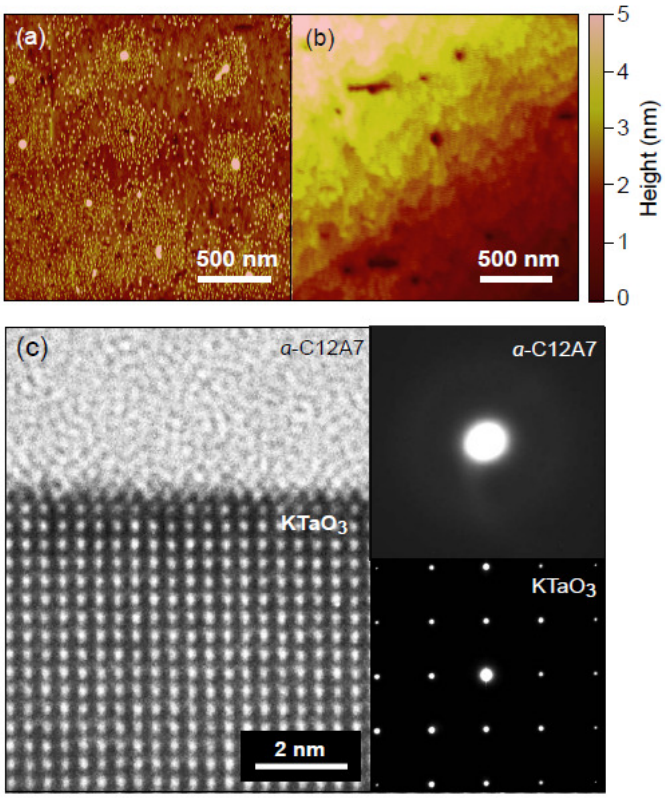

Fig.2: Topographic AFM images of (a) untreated and (b) BHF-treated $KTaO_3$ single-crystal surface. A smooth surface with steps and terraces is observed. (c) Cross-sectional HRTEM image of the 200-nm-thick *a*-C12A7/$KTaO_3$ heterointerface. An abrupt interface is visible. Selected area electron diffraction patterns of *a*-C12A7 and $KTaO_3$ are also shown.

deposited onto the stepped $KTaO_3$ surface by electron beam (EB, no substrate heating, base pressure ~10^{-4} Pa) evaporation through a stencil mask. Third, 200-nm-thick amorphous $12CaO{\cdot}7Al_2O_3$ (*a*-C12A7, permittivity ε_r = 12) glass film was deposited by a pulsed laser deposition (PLD, ~3 $Jcm^{-2}pulse^{-1}$, oxygen pressure ~0.1 Pa). It should be noted that *a*-C12A7 glass would be an appropriate gate insulator for $SrTiO_3$ and $KTaO_3$ as compared to *a*-Al_2O_3.[15,16] Finally, a 30-nm Ti film was deposited by EB evaporation as described above. In order to reduce the off current, the FETs were annealed at 150 ºC in air. Transistor characteristics of the resultant $KTaO_3$ FETs were measured by using a semiconductor device analyzer (B1500A, Agilent Technologies) at room temperature.

Results

Figure 2(c) shows a cross-sectional high-resolution transmission electron microscope image of the *a*-C12A7/$KTaO_3$ interface region (HRTEM, TOPCON EM-002B, acceleration voltage 200 kV, TOPCON). The featureless *a*-C12A7 (upper part) is observed, although the $KTaO_3$ layer exhibits a lattice (lower part). A broad halo is seen in the selected area electron diffraction patterns of *a*-C12A7, indicating that amorphous *a*-C12A7 film was deposited on the $KTaO_3$ layer.

Figure 3 summarizes typical transistor characteristics, such as transfer characteristics, field-effect mobility, sheet charge concentration, and the output of these FETs. The drain current (I_d) of the $KTaO_3$ FET increased markedly as the gate voltage (V_g) increased, hence the channel was *n*-type, and electron carriers were accumulated by positive V_g [Fig. 3(a)]. Relatively large hysteresis (~1 V) in I_d was also observed, most likely due to traps (~10^{12} cm^{-2}) at the *a*-C12A7/$KTaO_3$ interface. The on-off current ratio and the S-factor were >10^5 and ~1.2 $Vdecade^{-1}$, respectively. The threshold gate voltage (V_{th}), obtained from a linear fit of the $I_d^{0.5}$-V_g plot [Fig. 3(b)], was +5.2 V.

Using the above measured values, we calculated the sheet charge concentration (n_{xx}) and the field-effect mobility (μ_{FE}) of the $KTaO_3$ FETs. The n_{xx} values were obtained from $n_{xx} = C_i(V_g - V_{th})$, where C_i was the capacitance per unit area (51 $nFcm^{-2}$). The μ_{FE} values were obtained from $\mu_{FE} = g_m[(W/L)C_i \cdot V_d]^{-1}$, where g_m

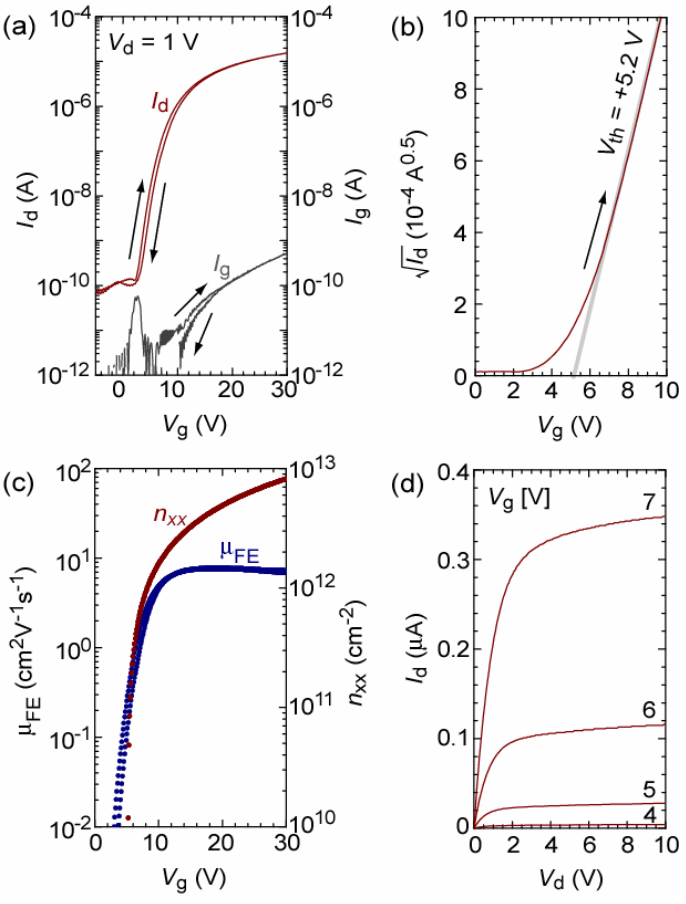

Fig.3: Typical transistor characteristics of a $KTaO_3$ FET with 200-nm thick *a*-C12A7 (ε_r=12) gate insulator at room temperature [(a) Transfer characteristic (I_d –V_g plot), (b) $Id^{0.5}$-V_g plot, (c) field-effect mobility (μ_{FE})-sheet charge density (n_{xx}) - V_g plots, (d) Output characteristic (I_d –V_d plot)]. The FET exhibits on-off current ratio ~10^5, sub-threshold swing *S*-factor ~1.2 V·decade-1 and threshold voltage V_{th} ~+5.2 V. The value of μ_{FE} increases drastically with V_g and reaches ~8 $cm^2V^{-1}s^{-1}$ or ~25% of the room temperature Hall mobility of electron-doped $KTaO_3$ (μ_{Hall} ~30 $cm^2V^{-1}s^{-1}$).

was the transconductance $\partial I_d / \partial V_g$. As shown in Fig. 3(c), μ_{FE} of the FET increased drastically with V_g and reached ~8 $cm^2V^{-1}s^{-1}$, which is ~25% of the room temperature Hall mobility of electron-doped $KTaO_3$ (μ_{Hall} ~30 $cm^2V^{-1}s^{-1}$). We also note that μ_{FE} of the $KTaO_3$ FETs were a factor of 4 greater than those of $SrTiO_3$ FETs, [13] most likely due to the difference in effective mass of the charge carrier m_e^* ($KTaO_3$: 0.13 m_0, $SrTiO_3$: 1.16 m_0). Furthermore, we observed a clear pinch-off and current saturation in I_d [Fig. 3(d)], indicating that the operation of this FET conformed to standard FET theory.

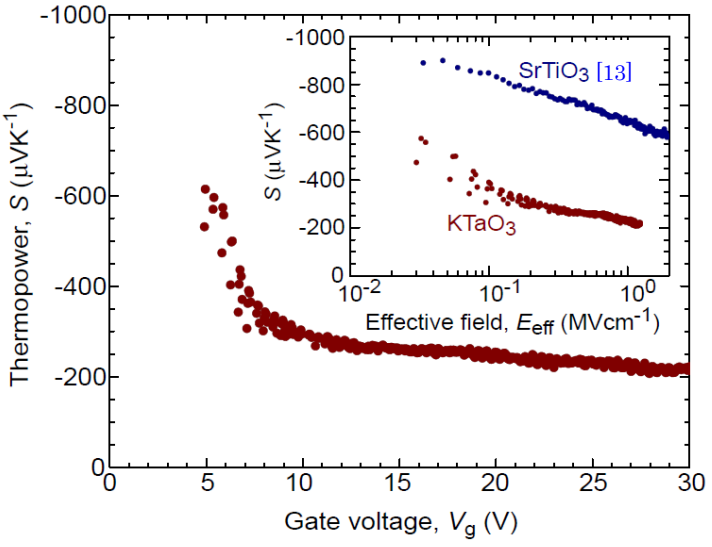

Fig. 4: Field-modulated thermopower (S) for the $KTaO_3$ FET channel. S for the $SrTiO_3$ FET channel (Ref. 13) is also plotted in the inset for comparison. Thermopower $|S|$ of the $KTaO_3$ FET is roughly ~400 μVK^{-1} smaller than that of $SrTiO_3$ FET and can be tuned from 600 to 220 μVK^{-1}.

Then, we measured field-modulated thermopower (S_{FE}) of the $KTaO_3$ FET. First, a temperature difference (ΔT = 0.2–1.5 K) was introduced between the source and drain electrodes by using two Peltier devices. Then, thermo-electromotive force (V_{TEMF}) was measured during the V_g-sweeping. The values of S were obtained from the slope of V_{TEMF}–ΔT plots. Figure 4 shows S_{FE}–V_g plots for the $KTaO_3$ FETs. The S_{FE}-values are negative, confirming that the channel is n-type. $|S|_{FE}$ gradually decreases from 600 to 220 μVK^{-1} by the application of gate electric field up to 1.5 $MVcm^{-1}$, due to the fact that n_{xx} increases with the V_g increases. These $|S|_{FE}$ values are approximately 400 μVK^{-1} lower than those for a $SrTiO_3$ FET as shown in the inset.[13] Since the value of $|S|_{FE}$ strongly depends on m_e^*, this result reflects the fact that m_e^* of $KTaO_3$ (0.13 m_0) is lower than that of $SrTiO_3$ (1.16 m_0).

Here we roughly estimate the maximum thermoelectric power factor ($PF = S \cdot \sigma$) of $KTaO_3$ at room temperature. The sheet conductance σ_{xx} of $KTaO_3$ was a factor of ~4 greater than that of $SrTiO_3$. The $|S|_{FE}$-value of $KTaO_3$ was 220 μVK^{-1}, while that of $SrTiO_3$ was 600 μVK^{-1} by the application of gate electric field up to 1.5 $MVcm^{-1}$. Thus, $S^2_{FE} \cdot \sigma_{xx}$ $KTaO_3$ / $S^2_{FE} \cdot \sigma_{xx}$ $SrTiO_3$ is ~0.5. Since the maximum $PF_{300\,K}$ of $SrTiO_3$ is ~3 $mWm^{-1}K^{-2}$,[17] $KTaO_3$ would exhibit maximum $PF_{300\,K}$ of ~1.5 $mWm^{-1}K^{-2}$, which corresponds well with the reported $PF_{300\,K}$ value (1.4 $mWm^{-1}K^{-2}$[4]).

Summary

We have fabricated single crystal $KTaO_3$-based field-effect transistors using amorphous $12CaO \cdot 7Al_2O_3$ glass gate insulator. The resultant FET exhibit excellent characteristics: on-off current ratio of ~10^5, sub-threshold swing S-factor of 1.2 $Vdecade^{-1}$, threshold gate voltage V_{th} of +5.2 V, and field effect mobility μ_{FE} of ~8 $cm^2V^{-1}s^{-1}$ (a factor of 4 greater than for $SrTiO_3$ FETs). The observed values of thermopower for the $KTaO_3$ FETs were ~400 μVK^{-1} below those of $SrTiO_3$ FETs, clearly demonstrating the difference of carrier effective mass m_e^*($KTaO_3$: 0.13 m_0, $SrTiO_3$: 1.16 m_0). The thermoelectric power factor $S^2 \cdot \sigma$ of $KTaO_3$ was estimated to be ~1.5 $mWm^{-1}K^{-2}$ at room temperature, which is approximately 50 % for that of

$SrTiO_3$, demonstrating the effectiveness of FET structure for the rapid exploration of thermoelectric materials.

Acknowledgments

A part of this work was financially supported by MEXT (Nano Materials Science for Atomic-scale Modification, 20047007).

References

[1] T. M. Tritt, M. A. Subramanian, H. Bottner, T. Caillat, G. Chen, R. Funahashi, X. Ji, M. Kanatzidis, K. Koumoto, G. S. Nolas, J. Poon, A. M. Rao, I. Terasaki, R. Venkatasubramanian and J. Yang, MRS Bull. (special issue on harvesting energy through thermoelectrics: power generation and cooling) **31**, 188 (2006) & articles therein.
[2] I. Terasaki, Y. Sasago and K. Uchinokura, Phys. Rev. B **56**, R12685 (1997).
[3] H.Ohta, Mater. Today **10**, 44 (2007).
[4] A. Sakai, T. Kanno, S. Yotsuhashi, H. Adachi and Y. Tokura, *Jpn. J. Appl. Phys*. **48** 097002 (2009).
[5] W. S. Baer, *J. Phys. Chem. Solids* **28**, 677 (1967).
[6] W. R. Hosler and H. P. R. Frederikse, *Solid State Commun*. **7**, 1443 (1969).
[7] M. Tsukioka, J. Tanaka and Y. Miyazawa, *J. Phys. Soc. Jpn*. **46**, 1785 (1979).
[8] G. O. Deputy and R. W. Vest, *J. Am. Ceram. Soc*. **61**, 321 (1978).
[9] V. F. Shamrai, A. V. Arakcheeva, V. V. Grinevich and A. B. Mikhailova, *Cristallogr Rep+*. **50**, 779 (2004).
[10] S. H. Wemple, *Phys. Rev. A* **137**, 1575 (1965).
[11] O. N. Tufte and P. W. Chapman, *Phys. Rev.* **155**, 796 (1967).
[12] H. P. R. Frederikse, W. R. Thurber and W. R. Hosler, *Phys. Rev*. **134**, A442 (1964).
[13] H. Ohta, Y. Masuoka, R. Asahi, T. Kato, Y. Ikuhara, K. Nomura and H. Hosono, *Appl. Phys. Lett*. **95**, 113505 (2009).
[14] M. Kawasaki, K. Takahashi, T. Maeda, R. Tsuchiya, M. Shinohara, O. Ishiyama, T. Yonezawa, M. Yoshimoto and H. Koinuma, *Science* **266**, 1540 (1994).
[15] K. Ueno, I. H. Inoue, T. Yamada, H. Akoh, Y. Tokura and H. Takagi, *Appl. Phys. Lett.* **84**, 3726 (2004).
[16] K. Ueno, I. H. Inoue, H. Akoh, M. Kawasaki, Y. Tokura and H. Takagi, *Appl. Phys. Lett.* **83**, 1755 (2003).
[17] H. Ohta, K. Sugiura and K. Koumoto, *Inorg. Chem*. **47**, 8429 (2008).